Focused Ion Beam Milling of Brass for Microinjection Mould Fabrication

Nikola Vladov[1], Svetan Ratchev[2], and Joel Segal[3]

[1]Nikola Vladov; Precision Manufacturing Centre, University of Nottingham; e-mail: epxnv2@nottingham.ac.uk•
[2]Svetan Ratchev; Precision Manufacturing Centre, University of Nottingham; e-mail: svetan.ratchev@nottingham.ac.uk
[3]Joel Segal; Precision Manufacturing Centre, University of Nottingham; e-mail: joel.segal@nottingham.ac.uk

ABSTRACT

In this paper focused ion beam (FIB) milling (sputtering) is demonstrated for the fabrication of brass microinjection moulding inserts which have been previously conventionally milled. It is found that FIB milling of the α phase of the material results in much smoother final surfaces than the β phase. An annealing procedure for minimizing the effects of differential sputtering has also been performed. Further with the help of Scanning Electron Microscopy (SEM) and White Light Interferometry (WLI) measurements the FIB milling yield for 70-30 cartridge brass is determined and analysed. Finally, FIB milling of 5µm square trenches with a flat bottom surface is demonstrated.

INTRODUCTION

Classical manufacturing techniques for hard material injection moulding inserts such as milling are currently restricted to approximately 25µm [1] and involve certain risk of expensive cutting tools breakage. Traditionally employed manufacturing methods for micro-inserts are the different LIGA based technologies, micro electro discharge machining (EDM), a variety of lithography (etching) techniques and laser ablation systems [2]. A disadvantage of these methods is that not all of them are capable of producing real 3D structures and they are applicable only to specific materials in different size ranges from 0.1µm to 100µm. An alternative proposed method is to take advantage of the Focused Ion Beam (FIB) instrument, traditionally used in materials science for TEM specimen preparation, failure analysis and mask repair in the semiconductor industry. FIB milling is possible for virtually any material and geometry and covers a wide size range from 50nm up to 25µm restricted by longer machining time. Therefore in this study classical milling (cutting) is combined with FIB milling (sputtering) to produce microinjection moulding inserts. Brass is chosen for this application as its mechanical properties meet the requirements of microinjection moulding processes and at the same time its hardness is lower than the commonly used steels hence decreasing the possibility of cutting tool breakage. Because of its excellent machinability improved by the addition of Pb the multiphase α-β brass alloy CZ121 is the primary choice for initial experiments. However, FIB milling of the material results in unacceptably rough final surfaces due to different sputtering rates for different grain orientations, preferential sputtering of elements with lower binding energy and cone formation.

The variation of the sputtering rate with the grain orientation is explained with the so called channelling effect. Along certain crystallographic directions the bombarding ions can penetrate deeper into the crystal leading to a reduced sputtering rate. This way different grains are milled with different speeds causing an uneven surface. Preferential sputtering of some elements of the alloy over others can be explained either by the larger probability of the lighter atoms being hit by an incoming ion or by the different surface binding energy for different elements. In both cases the surface layers of the machined target are enriched to the element with lower sputtering rates [3]. Cone formation was first reported in the 1950's and although since then many authors tried to explain the phenomenon there is no available satisfactory explanation to date. Cones can form from ridges, jags and other asperities related to the grain boundaries or microscopic impurities in the crystal structure including implanted ions from the ion beam itself. The motive power for cone growing can be preferential sputtering caused by the impurities or induced stress and amorphization of the crystal structure on the surface followed by complicated diffusion processes [4-8].

Unfortunately, existing methods of smoothing the machined surface in copper device editing [9] that rely on increasing the sputtering yield ratio between the copper lines and the underlying isolators are not applicable in the case of micromould insert fabrication.
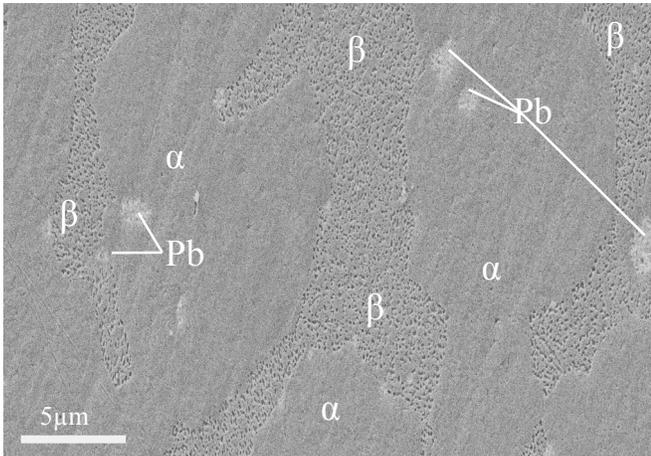
The objectives of this study are to find a new process for avoiding differential sputtering, to isolate the cone formation and to investigate the FIB milling yields for brass. To achieve these objectives the following techniques are employed: energy-dispersive X-ray spectroscopy (EDX) to identify the α and β phases of the alloy; scanning electron microscopy (SEM) for visual inspection; heat treatment for control of the grain sizes of the material; White Light Interferometry (WLI) to confirm the SEM measurements and determine the FIB milling yield.

EXPERIMENTAL PROCEDURES AND RESULTS

A. MATERIAL SELECTION AND SAMPLE PREPARATION

The initially chosen brass alloy CZ121M because of its excellent machinability is a mixture of two phases: alpha (α) and beta (β). The α phase contains up to 35% Zn and has face-centred cubic crystal structure whilst the β phase is in body-centred cubic structure and contains up to 50% Zn. Both phases are balanced with Cu and few percent of Pb which

• corresponding author

Fig. 1: SEM micrograph of the alloy CZ121 after mechanical polishing

Fig. 2: SEM micrographs at 30 deg tilt of two pockets milled in the alloy CZ121 under identical conditions but in different phases

improves the mechanical properties. Due to the different structure, different FIB milling behaviour can be expected. In order to discriminate between the phases EDX measurements from selected areas of the sample are performed. In Fig. 1, a SEM micrograph of the alloy CZ121 after mechanical polishing, it can be seen that the β phase is porous whereas the α is solid and free of macro defects. The Pb is found to segregate in separated grains and it can be expected that at the microscale it does not contribute to better machinability of the alloy. In Fig. 2, two pockets milled under identical beam parameters but on different phases of the alloy, α on the left and β on the right, are captured at 30 deg tilt. Cones are clearly distinguished on the surface of the porous β phase whilst the only defects on the α phase are the asperities due to differential sputtering. Although the Zn and the Cu have similar atomic weight their surface binding energy is in the ratio of approximately three to one so depletion of Cu due to preferential sputtering can be expected in the near-surface layer [10]. However, it is hard to judge how this influences the quality of the FIB milled surfaces.

Consequentially, taking in to account the segregation of the Pb and the milling properties of the two phases of the material, further experiments are done with Pb free single α phase 70-30 cartridge brass instead of the CZ121 alloy.

The defects caused by differential sputtering on the α phase are minimized by modelling the microstructure of the alloy. Following heat treatment procedures from the literature [11] the as supplied 70-30 cartridge brass is kept at 900 ºC for 45 min and then air cooled. Using standard ASTM tables the grain size of the annealed alloy is determined to be 213µm which is about two orders greater than the untreated material. This allows FIB milling to take place with very high probability on a single grain resulting in smooth final surfaces.

B. FOCUSED ION BEAM MILLING

To prove the concept trenches with target size 5x5µm are FIB milled on arbitrarily chosen grains from the surface of heat treated and mechanically polished 70-30 cartridge brass. All the work is carried out on a commercially available SEM/FIB CrossBeam workstation (NVision 40: Carl Zeiss SMT)
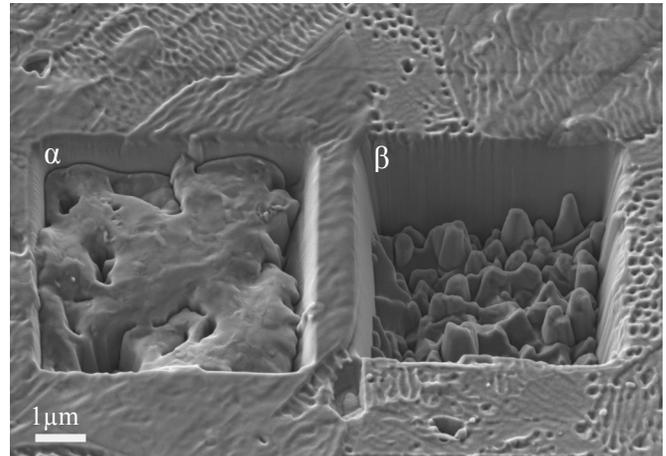
utilizing a beam of 30KeV Ga$^+$ ions. Scanning is performed in raster mode with three different beam currents of 0.3nA, 0.7nA and 1.5nA corresponding to spot size 38nA, 59nA and 107nA respectively. Varying the magnification the pixel overlap is kept at 160% and the dwell time is fixed to 53µs. Exposure time is set to 60s for all the trenches and the incidence angle is 0 deg. In Fig. 3 a SEM micrograph of one of the series of the sputtered trenches is shown. Under these processing parameters with this material the cones do not form and the asperities due to differential sputtering are not observed. The only defects that can be noticed are the small "wavelike" patterns on the bottom of the trenches' final surfaces which need further investigation. The quality of the machined surfaces appears not be influenced by the magnitude of the beam current. Quantitative roughness measurements are prevented by the non standard "wavelike" patterns. Single measurements using the analyzing functions of the SEM show the features to be within 50nm of the aimed size and again not depending on the beam current. The error is less than 1% and should be considered more like a tool calibration problem than reproduction incapability. Fig. 3 shows slight distortion caused by the tilt correction function (the sample is at 30deg relative to the beam).

C. MILLING YIELD MEASURMENTS
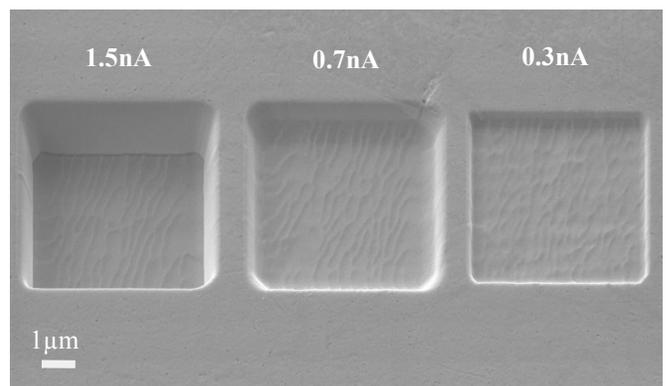
Fig. 3: SEM micrographs at 30 deg tilt of three trenches milled with different currents in a single grain of the 70-30 cartridge brass
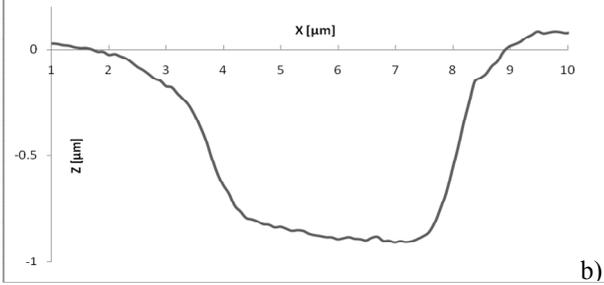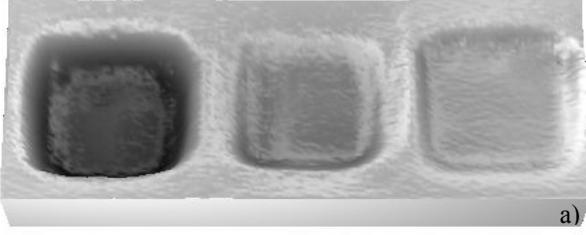
Fig.4: a) a 3D plot of the milled features and b) typical profile of the middle trench obtained by WLI

A precondition for accurate fabrication of the micromould insert is knowledge of the FIB milling yield Y of the heat treated 70-30 cartridge brass. Measurements are done in cubic micrometres per nanocoulomb ($\mu m^3/nC$) using the following equation:

$$Y = \frac{A \times h}{I \times t} \quad (1)$$

where A and h are the area and the depth of the milled feature in μm, I is the beam current in nA and t is the exposure time in seconds. The depth of the trenches from Fig.3 is primarily determined using the SEM and confirmed independently by WLI measurements in VSI mode performed on a VEECO NPFlex instrument. A 3D plot of the features and typical profile of the middle trench are presented in Fig. 4. Due to the poor optical resolution of the interferometer the overall shape is not well captured. However, the resolution in the vertical direction is quoted to be better than 0.15nm; the results are summarized in Table 1. The yield increases with the higher values of the current which at first glance seems to be in contradiction of other published works. To analyze this problem a model proposed by Santamore et al. [12] is applied which gives the dependence of the yield Y on the local incidence angle θ:

$$Y^c(\theta) \propto \frac{v \times \tan(\theta)}{J} \quad (2)$$

where v is the beam linear speed and J is the current density. $Tan(\theta)$ can be approximated as the ratio between the depth of the trench achieved after single pass (loop) of the beam h^s and the beam spot size d. Although J follows Gaussian distribution radial to the centre point in order to simplify the calculations in the present paper it is considered to be uniform across the whole radius. It must be noted that change of current is always followed by change of the spot size and since the dwell time and pixel overlap are fixed the scan speed also changes inevitably. In Table 1 the required calculation data together with the results are presented. The values obtained for the theoretical yield are normalized to 0.776 so that easy

Table 1: Calculated and measured milling yield for different beam currents, including the model related data

current I [nA]	0.3	0.7	1.5
spot size d [μm]	38	59	107
current density J [$nC/\mu m^2$]	66	64	61
beam speed v [$\mu m/s$]	452	693	1285
depth h [μm]	0.354	0.949	0.560
number of beam loops	27	63	214
single loop depth h^s[nm]	13.19	15.06	13.04
local angle θ [deg]	19	14	7
calculated yeld Y^c [arb. unit]	0.490	0.571	0.776
measured yeld Y [$\mu m^3/nC$]	0.491	0.565	0.776

comparison to the experimental values can be done. In spite of the approximations the calculated yield follows exactly the same trend as the measured. However, the model does not take in to account the redepostion effects which will become dominant below a certain value of the scan speed and the contrary situation will be observed- decrease of the yield with increase of the current.

Since the above results are for an arbitrary chosen grain before proceeding to actual machining further experiments to relate the milling yield to the crystal orientation are needed. This can be done using an Electron Back Scattered Diffraction (EBSD) detector attached to the CrossBeam instrument. Nevertheless, Fig. 5 represents a uniformly milled pattern at the boundary between two grains which shows that in certain orientations the milling rate is kept constant.

CONCLUSIONS AND FURTHER DEVELOPMENT

1. It is found that within the investigated process parameters cones appear only on the β phase brasses hence α phase brasses are more suitable for FIB milling.

2. It is demonstrated that the grain size of 70-30 cartridge brass can be controlled by heat treatment in such a way that effectively FIB milling is performed in a single crystal structure.

3. The quality of the FIB milled surfaces is not dependant on the beam current within the investigated process parameters.

4. It is shown how the milling rate for 70-30 cartridge brass can be determined so that accurate fabrication of the micromould insert is possible.
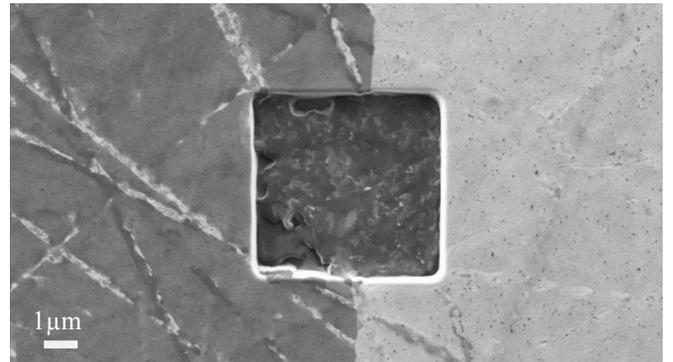

1μm

Fig.5: Channelling contrast FIB image of pattern milled at the boundary of two grains

5. The added lead in brass alloys segregates in separate grains thereafter it is assumed that it does not improve the machinability of the material in microscale.

6. Further experiments with included EBSD analysis are needed to relate the milling yield to the crystal orientation.

ACKNOWLEDGMENTS

REFERENCES

[1] G. L. Benavides, L. F. Bieg, M. P. Saavedra, and E. A. Bryce, "High aspect ratio meso-scale parts enabled by wire micro-EDM," *Microsystem Technologies,* vol. 8, no. 6, 2002, pp. 395-401.

[2] J. Giboz, T. Copponnex, and P. Mele, "Microinjection molding of thermoplastic polymers: a review," *Journal of Micromechanics and Microengineering,* vol. 17, no. 6, 2007, pp. R96-R109.

[3] M. Nastasi, J. Mayer, and J. Hirvonen, Ion- solid interactions: fundamentals and applications, Editor: 1996, pp.229-235.

[4] G. K. Wehner, "Cone formation as a result of whisker growth on ion bombarded metal-surfaces," *Journal of Vacuum Science & Technology a-Vacuum Surfaces and Films,* vol. 3, no. 4, 1985, pp. 1821-1835.

[5] R. S. Robinson, and S. M. Rossnagel, "Ion-beam-induced topography and surface-diffusion," *Journal of Vacuum Science & Technology,* vol. 21, no. 3, 1982, pp. 790-797.

[6] G. Carter, B. Navinšek, and J. Whitton, "Heavy ion sputtering induced surface topography development," *Sputtering by Particle Bombardment II*, 1983, pp. 231-269.

[7] N. G. Shang, X. L. Ma, C. P. Liu, I. Bello, and S. T. Lee, "Arrays of Si cones prepared by ion beams: growth mechanisms," *Physica Status Solidi a-Applications and Materials Science,* vol. 207, no. 2, 2010, pp. 309-315.

[8] L. B. Begrambekov, A. M. Zakharov, and V. G. Telkovsky, "Peculiarities and mechanism of the cone growth under ion bombardment," *Nuclear Instruments & Methods in Physics Research Section B-Beam Interactions with Materials and Atoms,* vol. 115, no. 1-4, 1996, pp. 456-460.

[9] B. W. Kempshall, S. M. Schwarz, B. I. Prenitzer, L. A. Giannuzzi, R. B. Irwin, and F. A. Stevie, "Ion channeling effects on the focused ion beam milling of Cu," *Journal of Vacuum Science & Technology B,* vol. 19, no. 3, 2001, pp. 749-754.

[10] M. Szymonski, "Sputtering of Cu and Zn atoms from elemental and alloy targets," *Applied Physics,* vol. 23, no. 1, 1980, pp. 89-92.

[11] R. S. French, "Grain growth and recrystallization of 70-30 cartridge brass," *Transactions of the American Institute of Mining and Metallurgical Engineers,* vol. 156, 1944, pp. 195-210.

[12] D. Santamore, K. Edinger, J. Orloff, and J. Melngailis, "Focused ion beam sputter yield change as a function of scan speed," *Journal of Vacuum Science & Technology B,* vol. 15, no. 6, 1997, pp. 2346-2349.